Smart Structures and Systems, *Vol. 31*, *No. 5* (*2023*) *455-467*
https://doi.org/10.12989/sss.2023.31.5.455

Experimental and numerical study on the dynamic behavior of a semi-active impact damper

Zheng Lu [1,2], Mengyao Zhou [1], Jiawei Zhang*[1], Zhikuang Huang [1] and Sami F. Masri [3]

[1] *Department of Disaster Mitigation for Structures*, *Tongji University*, *Shanghai*, *200092*, *China*
[2] *State Key Laboratory of Disaster Reduction in Civil Engineering*, *Tongji University*, *Shanghai*, *200092*, *China*
[3] *Viterbi School of Engineering*, *University of Southern California*, *Los Angeles*, *CA 90089-2531*, *USA*

(*Received October 2*, *2022*, *Revised February 25*, *2023*, *Accepted March 7*, *2023*)

Abstract. Impact damper is a passive damping system that controls undesirable vibration with mass block impacting with stops fixed to the excited structure, introducing momentum exchange and energy dissipation. However, harmful momentum exchange may occur in the random excitation increasing structural response. Based on the mechanism of impact damping system, a semi-active impact damper (SAID) with controllable impact timing as well as a semi-active control strategy is proposed to enhance the seismic performance of engineering structures in this paper. Comparative experimental studies were conducted to investigate the damping performances of the passive impact damper and SAID. The extreme working conditions for SAID were also discussed and approaches to enhance the damping effect under high-intensity excitations were proposed. A numerical simulation model of SAID attached to a frame structure was established to further explore the damping mechanism. The experimental and numerical results show that the SAID has better control effect than the traditional passive impact damper and can effectively broaden the damping frequency band. The parametric studies illustrate the mass ratio and impact damping ratio of SAID can significantly influence the vibration control effect by affecting the impact force.

Keywords: impact damper; mechanical model; numerical simulation; semi-active control; shaking table test

1. Introduction

In order to meet the functional requirements of the structure under undesirable excitations, vibration control approaches for engineering structures have been explored over the past century. The control approaches can be generally classified as passive, active, semi-active and hybrid control (Ledezma-Ramírez *et al*. 2019). The passive control approaches have been widely applied with the superiority of clear concept and easy implementation without external input energy. Energy dissipators, base isolators and tuned mass dampers, as representative passive control systems with different damping mechanisms, have been broadly studied and applied (Domizio *et al*. 2019, Nochebuena-Mora *et al*. 2021, Parulekar and Reddy 2009). Typically, the tuned mass damper (TMD), which consists of a mass block, a spring element and an energy-consuming component, has been proved to show an excellent damping performance in engineering structures worldwide (Elias and Matsagar 2017). However, defects exist inevitably in this type of linear damping system (Marano and Greco 2011). It is observed that TMD can only work efficiently in a narrow frequency range, and the large mass block and correspondingly working space will lead to higher costs in practical projects. Researchers have contributed a lot to solve the deficiencies of TMD by introducing the nonlinear mechanism. For example, inerters (Ma *et al*. 2021, Marian and Giaralis 2017), eddy-current TMD (Lu *et al*. 2017), nonlinear energy sink (NES) (Iurasov and Mattei 2020), shape memory alloys (SMA) (Gur *et al*. 2019) and nonlinear impact dampers (Gharib and Karkoub 2017) have been investigated to improve the damping performance of TMD.

Impact damper (ID), which can interfere with the amplitude accumulation process of the original structure by impact momentum exchanges between the mass block and main structure, has embodied its advantage of inexpensive implementation and efficient damping capacity under a broad frequency range (Gagnon *et al*. 2019). Song *et al*. (2016) proposed a pounding tuned mass damper integrated with TMD and ID, and it is proved that the nonlinear damping system can effectively suppress the vibration of pipeline structures attached. Xue's research (Xue *et al*. 2017) also indicated that the pounding tuned mass damper showed excellent performance in high-rise steel structures. On the other hand, particle damper was proposed substituting mass block with multi-particle to weaken the noise influence occurred during the impact process. Papalou and Masri (1998) conducted an in-depth study on the damping mechanism and equivalent simplification method of particle dampers through theoretical analysis and experimental studies. He *et al*. (2021) proposed a multiple unidirectional single-particle damper, which can reduce the structural response with limited working space. Lu *et al*. (2021) developed a particle tuned mass damper combining tuning and impact energy dissipation damping mechanisms.

*Corresponding author, Ph.D. Student,
E-mail: zhangjiawei9@tongji.edu.cn

Copyright © 2023 Techno-Press, Ltd.

ISSN: 1738-1584 (Print), 1738-1991 (Online)

It is found that impact damper and particle damper, as passive control approaches, cannot control the impact moment to ensure control stability through the feedback and control systems under complex and unpredictable external excitation.

The semi-active control approach was firstly proposed by Hrovat *et al*. (1983) subjected to environmental loads in the field of structural engineering, which can provide enhanced vibration suppression capacity. In contrast to passive and active control approaches, semi-active approaches derive their actuating forces from the motion of the structure itself, with suitably adjustable mechanical devices being used to provide the control forces. Semi-active approaches have become attractive in structural vibration control applications due to the controllable damping and the low power requirements to operate the damping device (Chung *et al*. 2013, Hgsberg 2011, Hwang *et al*. 2020, Lai *et al*. 2018, Poplawski *et al*. 2019, Soria *et al*. 2017, Wang *et al*. 2021). Sun and Nagarajaiah (2014) proposed a variable stiffness-variable damping semi-active tuned mass damper (STMD), they verified that STMD can effectively reduce the structural response under earthquake by tracking the motion states of the TMD and structure to adjust the damping and stiffness. Besides, it is found that the semi-active algorithm can be designed to replace the damping force with the controllable friction force so that the TMD and the main structure periodically generate a negative 90 degree phase difference to achieve the optimal vibration reduction effect of the lightweight TMD (Ferreira *et al*. 2019, Lai *et al*. 2018). Based on the impact damping mechanism, Lu *et al*. (2019) conducted a preliminary study on the semi-active implementation of the impact damper, and the effects of the damping system considering structural nonlinearity under strong earthquakes was investigated.

It is worth mentioning that semi-active strategies are required in semi-active control systems to achieve actuation forces similar to that of active control systems. However, it is difficult for the semi-active damping system to provide sufficient control force in practical engineering structures subjected to seismic excitations, and the slow response of the semi-active device makes it difficult to provide the right control force to the structure in time (Yang *et al*. 2002). Moreover, Ferreira *et al*. (2019) found in a comparative study that semi-active TMDs require only 1/5 of the original TMD mass in their design, but semi-active TMDs require a larger stroke and higher working space dimensions. The impact damper, which obtains the momentum and energy efficiently from the main structure by impacts, can start working and provide sufficient actuation force quickly in a limited working space. Therefore, it shows great potential in semi-active control approaches. Nevertheless, limited experimental research related has been reported, while most previous studies show concern for analytical studies. In this paper, a technical implementation of semi-active impact damper (SAID) whose impact gap-clearance can be adjusted according to a semi-active control strategy is established, and the damping performance is investigated and verified based on shaking table tests. A verified simulation model is designed to further study the damping mechanism of SAID.

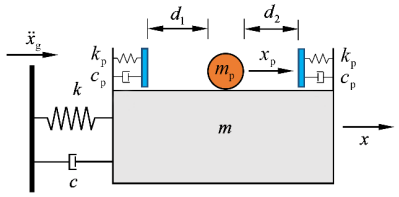

Fig. 1 The mechanical model of the SAID

The remaining of this paper is organized as follows: the semi-active strategy for the variable gap-clearance semi-active impact damper is proposed in Section 2. The setup of a single-floor frame structure shaking table test is introduced in Section 3. The experimental results of SAID controlled system are performed in Section 4. Section 5 presents the numerical simulation of the SAID attached structure and a series of parametric studies. Finally, conclusions are drawn in Section 6.

2. Semi-active control strategy of SAID

It is discovered that the impact damping system mainly attenuates the structural vibration through the momentum exchange during the collisions between the impact block and the main structure, and the momentum exchange is affected by their relative velocity. Harmful momentum exchange occurs in the case when the relative velocity is in the same direction as structural velocity. Therefore, a control strategy can be designed to control the impact timing to maximize the momentum exchange and improve the damping performance, and the SAID system with a variable gap-clearance is proposed based on the traditional passive impact damper concept.

The mechanical model applied to a single-degree-of-freedom (SDOF) structure is shown in Fig. 1, with the mass of the main structure as m, the stiffness coefficient as k, the damping coefficient as c and the displacement as $x(t)$. Similarly, the mass and the displacement of the mass block are expressed as m_p and $x_p(t)$, the stiffness and damping coefficient of the mass block between the baffle are k_p and c_p, respectively. The distances between the mass block from the left baffle and right baffle are d_1 and d_2, $d = d_1 + d_2$ is defined as the gap-clearance of the damper. The impact timing can be controlled by changing the baffles position to adjust d_1 and d_2 according to the semi-active control strategy in SAID.

The governing equation of SDOF structure with SAID attached is

$$\begin{cases} m\ddot{x} + c\dot{x} + kx - F_p - F_c = -m\ddot{x}_g \\ m_p\ddot{x}_p + F_p + F_c = -m_p\ddot{x}_g \\ F_p = c_pH(y,\dot{y}) + k_pG(y) \end{cases} \tag{1}$$

where the $\ddot{x}_g$ is the input excitation acceleration, x, $\dot{x}$, $\ddot{x}$ are the relative displacement, velocity and acceleration vectors of the main structure with respect to its base, respectively. $\ddot{x}_p$ is the acceleration of the mass block, F_p is the impact force produced by the impact between the mass block and the baffle, and F_c is the Coulomb friction force

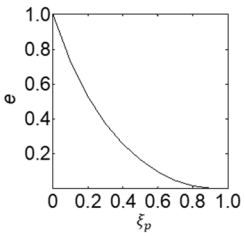

Fig. 2 Relationship of impact damping ratio ξ_p and restitution coefficient e

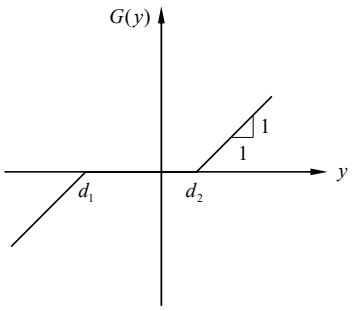

(a) Stiffness function

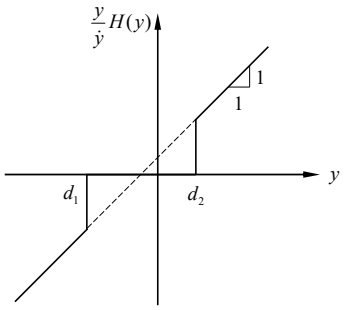

(b) Damping function

Fig. 3 Nonlinear functions

when the mass block moves between the baffles. $k_p = m_p\omega_p^2$ is impact stiffness coefficient, where the impact angular frequency ω_p is generally set as 20 times the structural angular frequency to simulate the elastic impact process, and $c_p = 2m_p\xi_p\omega_p$ is the impact damping coefficient in the inelastic impact process, where the damping ratio ξ_p is related to the restitution coefficient e of the material, the specific relationship is shown in Fig. 2. y, $\dot{y}$ are the relative displacement and velocity of the mass block to the main structure. $G(y)$, $H(y,\dot{y})$ are nonlinear functions for simulating the impact elastic force and damping force, which are shown in Fig. 3.

According to the research on the law of motion and momentum exchange of impact damping system in steady state (Masri *et al*. 1989), the impacts always happen when the velocity of structural top reaches maximum or the relative displacement of the top-bottom of the main structure returns to zero, and the momentum exchange is optimal at these moments. Considering that the control algorithm based on the structural velocity is more difficult to implement, it is a more reliable solution to control the impact timing of SAID based on the structural displacement.

The vibration control performance of the SAID-SDOF coupling system under harmonic excitation with different impact timings is discussed in Fig. 4 based on the structural response, accumulated input energy and dissipated energy (Lu *et al*. 2021), and the impact timing is determined by the structural displacement control point. In Fig. 4(a), the amplitudes of the structural energy and responses are normalized in the scenario where the displacement control point is 0.06mm, which represents the maximum values among the cases studied. It is found that when the displacement control point is zero, the ratio of accumulated dissipated energy to external input energy is maximum, while the responses and the energy of the controlled structure are minimum meanwhile. Consequently, a semi-active control strategy of SAID is proposed as follows:

(1) The impacts happen at the moment when the relative displacement of the top-bottom of the main structure returns to zero, in order to maximize the momentum exchange in each impact.
(2) When an impact occurs, the relative velocity direction of the top-bottom of the main structure should be opposite to the velocity direction of the mass block moving relative to the top of the main structure to avoid harmful momentum exchange.

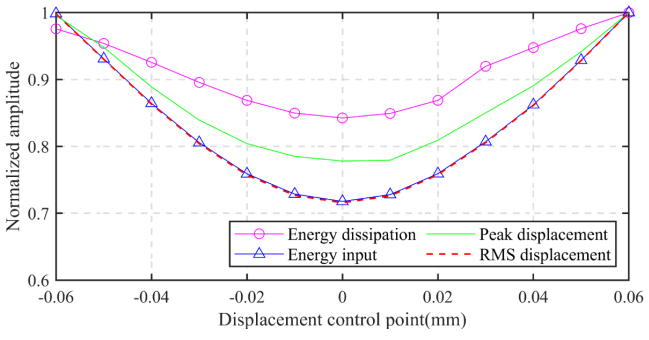

(a) Energy and displacement response of the main structure

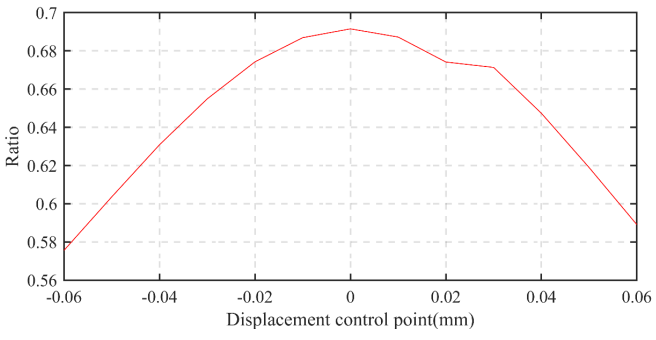

(b) Ratio of accumulated dissipated energy to external input energy

Fig. 4 Effect of different displacement control points on SAID damping effect

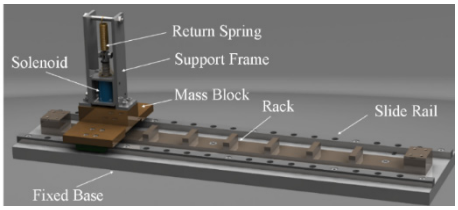

(a) After assembling

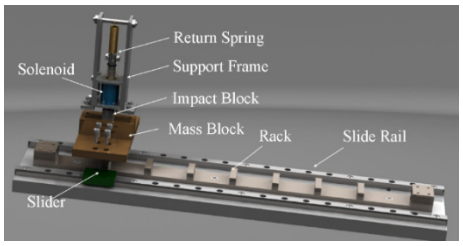

(b) Before assembling

Fig. 5 SAID machinery diagram

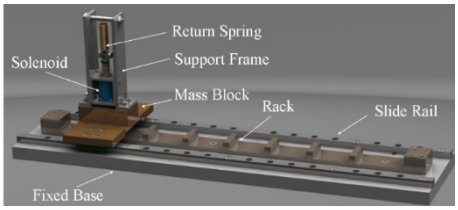

(a) After assembling

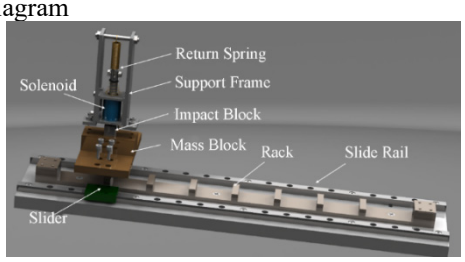

(b) Before assembling

Fig. 5 SAID machinery diagram

3. Shaking table test setup

3.1 SAID device

The technical implementation of SAID consists of the machinery device and the real-time monitoring feedback system. SAID machinery adopts the design that the retractable impact block collides with the racks to realize the position changes of the movable baffles instead of the uninterrupted moving baffle, the latter places higher demands on the stability of the control system and larger external energy input.

The SAID machinery device is shown in Fig. 5. The mass block fixed to the slider is free to move on the slide rail and collides with the boundary protruding from the end to limit its motion range. The electromagnetic control device mounted on the impact block is the key for the semi-active control, including the support frame, return spring, solenoid and impact block, and the impact block can be moved up and down through the square hole in the center of the mass block. While the mass block and electromagnetic control device move in the same direction at a certain moment, the semi-active control program, if it determines that an impact is required and issues a command to energize the electromagnet, the impact block will move downward and collide with the rack. Then the mass block moves in the opposite direction, and the impact block separates from the rack. At this moment, the control procedure will issue a command to disconnect the solenoid to restore the impact block inside the mass block.

In order to enable the electromagnetic control device to realize the control of impact timing, a real-time monitoring feedback system is built, which can collect and process the displacement response data of the main structure as well as the mass block through the laser displacement sensor, while judging whether to release the corresponding command through the semi-active control algorithm. The workflow of the real-time monitoring feedback system with the mechanical device is shown in Fig. 6.

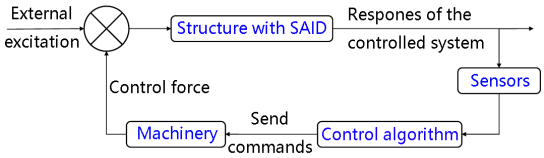

Fig. 6 SAID real-time monitoring feedback system workflow diagram

The time lag of this system is mainly from the delay between the command issued by the control program and the completion of the solenoid action, which can be obtained by high-speed camera shooting and projection. The state prediction compensation mechanism for SAID is proposed to reduce the time lag effect on the control accuracy. Specifically, the real-time monitoring feedback system collects and stores the displacement response data of the main structure and the mass block at a constant frequency. The control program can use these data to calculate the current speed and acceleration of the main structure and the mass block, then predict the position of the main structure and the mass block after a certain time interval. The control program can release corresponding commands at the most suitable time to ensure the realization of the semi-active control strategy.

In the shaking table test, the fixed base and the mass block of the SAID machinery device are made of lightweight acrylic plate. The total mass of the movable part consisting of the mass block and the electromagnetic control device is 0.206 kg. The distance between the impact boundary on both sides of the slide rail is 375 mm, and the width of the rack is 25 mm. 9 racks are evenly arranged in the rail with a rack pitch of 40 mm. The control program of the real-time monitoring feedback system collects and stores displacement data at 25 Hz. The time lag between the power-on command and the electromagnet pushing the

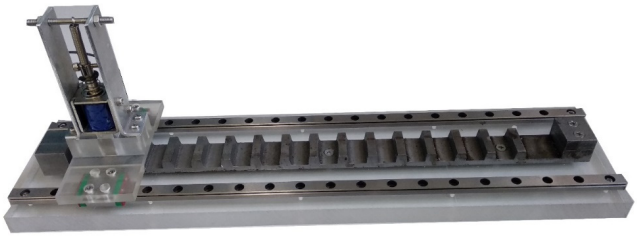

(a) SAID machinery device

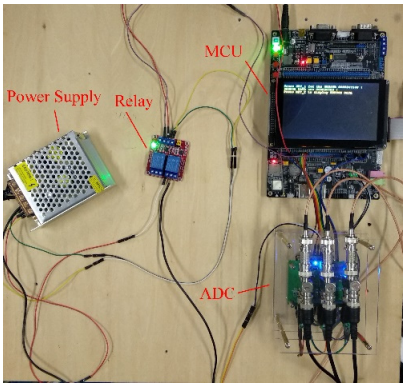

(b) Data acquisition and feedback control system

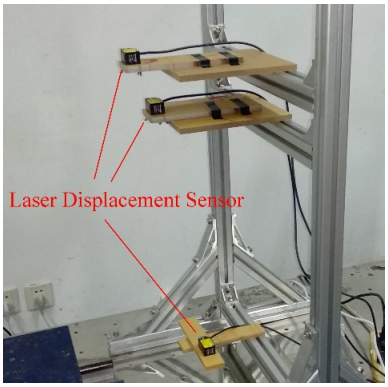

(c) Laser displacement sensor arrangement

Fig. 7 Technical implementation of SAID in the test

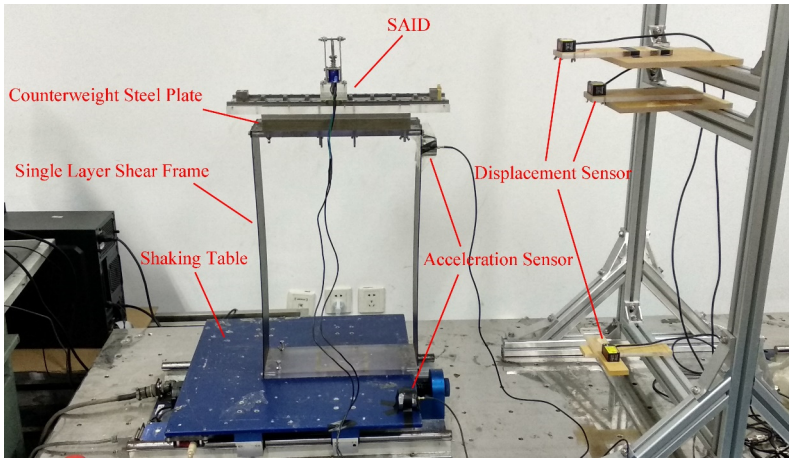

Fig. 8 Configuration of the test structure

impact block down to the impact position is about 0.033 s, and the time lag between the power-off command and the reset spring pulling the impact block back to the original position is about 0.021 s. The photos of the machinery device and real-time monitoring feedback system in the test are shown in Fig. 7.

3.2 Shear frame structure model

The shaking table test was carried out using a single-floor shear frame model, as shown in Fig. 8. The frame size is 320 mm × 110 mm × 500 mm, the top mass is 0.75 kg. The fixed base of SAID is installed on the top of the frame, counterweight steel plate and acceleration sensor are used as additional mass, leading to the total mass of the structure top-floor with 9.13 kg.

3.3 Test condition design

The shaking table works with a maximum travel distance of ±7.5 cm and a frequency of 0-20 Hz, and the maximum velocity and acceleration are 83.8 cm/s and 24.5 m/s^2, respectively. The main test conditions used in this test are shown in Table 1, and the SAID mass ratio is set as 2.26%.

During the test, the single-floor shear frame structure was first subjected to a free vibration to explore its dynamic characteristics and initially examine the damping effect of SAID. Then the shaking table tests for the frame structure with SAID attached were conducted under the resonant harmonic wave and the seismic excitations respectively. The seismic excitations used are El Centro wave and 14 randomly selected seismic waves. In addition, to compare

Table 1 Test conditions

No.	Group	Control Method	Excitation Type	Amplitude(g)
1	A1	Uncontrolled	Initial displacement 25mm	/
2	A2	Uncontrolled	Initial displacement 50mm	/
3	A3	SAID	Initial displacement 50mm	/
4~14	B1~B11	SAID	Harmonic wave	0.005~0.015(0.001)
15~25	C1~C11	SAID	El Centro	0.05~0.15(0.01)
26~36	D1~D11	ID (d = 45mm)	El Centro	0.05~0.15(0.01)
37~47	E1~E11	ID (d = 83mm)	El Centro	0.05~0.15(0.01)
48~61	F1~F14	SAID	14 randomly selected seismic waves	0.08

(a) Time history curve (b) Amplitude spectrum

Fig. 9 Displacement response of uncontrolled structure at an initial displacement of 25 mm

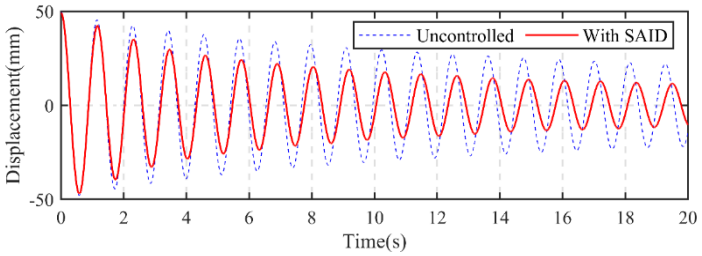

Fig. 10 Comparison of displacement time history of uncontrolled structure and structure with SAID attached

the damping performance of SAID and ID, shaking table tests under El Centro wave were conducted for IDs with gap-clearances d of 45 mm and 83 mm, respectively. The excitation amplitude in the test increases in equal intervals, and the values of the intervals are shown in the brackets in the rightmost column of the table.

4. Experimental results analysis

4.1 Free vibration

The displacement time-history curve and the displacement amplitude spectrum of the single-floor shear frame with the accelerometer, counterweight plate and the SAID base installed for free vibration under the applied 25 mm initial displacement are shown in Fig. 9. The damping ratio of the frame structure is 0.014, and the natural frequency is 0.891 Hz, which is close to that of typical high-rise building structures.

The displacement time-history curves of the uncontrolled structure and the SAID controlled structure for free vibration with an applied initial displacement of 50 mm, are shown in Fig. 10. It can be seen that SAID can work efficiently to enable the structural displacement response to decay faster.

4.2 Harmonic excitation

The damping effect of SAID in normal and extreme working conditions under resonant harmonic excitation with an excitation frequency ratio of 1.0 for different acceleration amplitudes is shown in Fig. 11. The peak and root-mean-square (RMS) response reduction ratios are investigated as indices. The structural displacement and acceleration control effect of SAID under resonant harmonic excitation with an amplitude of 0.011g and lower is generally efficient and stable in normal working conditions.

When the excitation intensity is higher and SAID attached to the structure works in an extreme condition, the relative velocity between the mass block of SAID and the main structure increases. In this case, the mass block is more likely to collide with the boundary of the slide rail

(a) Displacement (b) Acceleration

Fig. 11 Vibration reduction ratios of structural peak response and root-mean-square response at different acceleration amplitudes

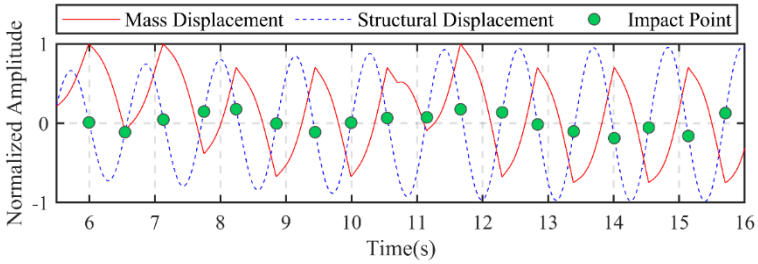

(a) 0.005 g

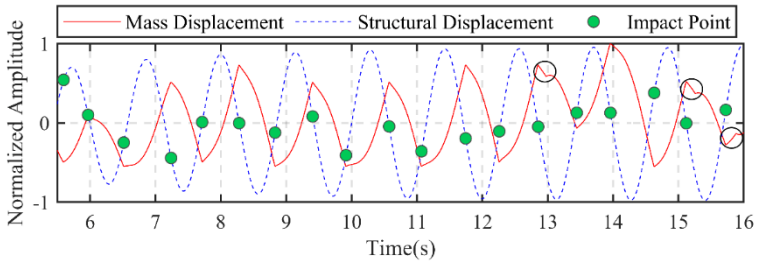

(b) 0.015 g

Fig. 12 Analysis of impact points at different input acceleration amplitudes

before the structural displacement returns to zero, leading to worse control accuracy in extreme working conditions. On the other hand, the mass block velocity is faster after a collision and the impact block is more likely to have a harmful impact on the adjacent rack during the period between the power-off command from the semi-active control program and the return of the impact block to its original position.

To further investigate the implementation of SAID control strategy, the relative displacement of the mass block to the structural top, the structural displacement and the impact point (the main structure displacement when the impact occurs) under different input acceleration amplitudes are analyzed and shown in Fig. 12. When the impacts occur, the velocity direction of the main structure is opposite to the velocity direction of the mass block moving relative to the top of the main structure, which is consistent with the semi-active control strategy. When the acceleration amplitude is 0.005 g with a normal working condition, the impact points are basically concentrated near the zero point of the structure displacement. However, when the acceleration amplitude is 0.015 g with an extreme working condition, the impact points become very scattered and the control accuracy of SAID decreases significantly. By analyzing the displacement time history of the mass block relative to the top of the main structure under different working conditions, it was found in the test that when the input acceleration amplitude reaches 0.012 g, the number of collisions between the mass block and the boundary starts to increase significantly, making it difficult to keep the impact point near the zero point of structural displacement, and the damping effect of SAID decreases significantly at this time.

When the acceleration amplitude is 0.015 g, three circle marked depressions can be observed on the relative displacement time history curve of the mass block in Fig. 12(b), indicating that the impact block is not restored to its original position in time after the normal collision due to the excessive bounce speed, and the harmful impact happens between the impact block and adjacent rack. In this comparison study of the normal working and extreme conditions of SAID under resonant harmonic excitation, it

can be seen that the SAID in the test can execute the preset semi-active control strategy well, but the insufficient design travel of the SAID machinery limits the control effect of the SAID. In order to prevent the undesirable impacts with the boundary and adjacent rack in the extreme conditions in the practical case, approaches can be adopted to improve the SAID damping performance subjected to the strong excitation by properly extending the length of the slide rail and increasing the friction between the slider and the rail.

4.3 Comparison of damping performance for SAID and ID under seismic excitations

The SAID can be converted to an ID machinery with fixed clearances by installing a fixed baffle, as shown in Fig. 13. Changing the position of the baffle can obtain IDs with a gap-clearance of 45 mm and 83 mm based on the shape characteristics of the machinery.

Fig. 14 displays the displacement time history of the uncontrolled structure as well as structures with various damping systems subjected to the El Centro wave with an acceleration amplitude of 0.10 g. As shown in Fig. 14(a), the SAID system is capable of effectively mitigating the structural displacement response, exhibiting efficient damping performance during the 20~35 s period. Fig. 14(b)compares the damping effects of SAID and ID with different gap-clearances. The SAID system demonstrates superior peak response attenuation compared to the passive ID system. On the other hand, for the passive control system, the ID with an 83 mm gap-clearance shows better damping effects.

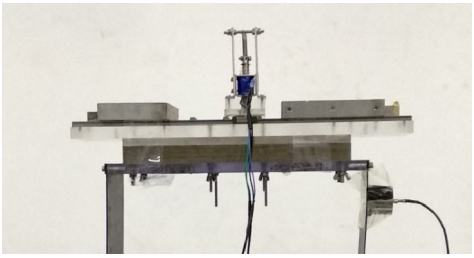

Fig. 13 ID machinery in the shaking table test

Fig. 15 further shows the damping effects of SAID and ID with different gap-clearances for the SDOF structural displacements under El Centro wave with different acceleration amplitudes. It can be seen that SAID generally shows the best damping performance, while ID with a gap-clearance of 45 mm is the worst. When the input excitation acceleration amplitude is 0.05 g, the three dampers all work steadily and the damping performances is close. With the increase of acceleration amplitude, the damping effects of both passive IDs have a significant decrease, and the changing trend of the damping effect of the two is very similar. In comparison, the damping effects of SAID on the peak and RMS displacement are more stable by controlling the gap-clearance and impact timing, indicating that SAID can keep working efficiently in the normal working condition in high-intensity seismic excitation.

With the increase of the structural response caused by the incremental input acceleration amplitude, the damping system with fixed clearance cannot control the motion of the mass block, and the harmful impacts increase, leading to less effective momentum exchange and worse damping performance. The SAID system with the introduction of the semi-active control strategy can monitor the motion status of the main structure and the mass block in real time and control the mass block to collide at the right time, so as to avoid harmful impacts while improving the momentum exchange of each impact. Therefore, the damping performance of SAID shows better robustness in the face of seismic excitation with varying acceleration amplitudes.

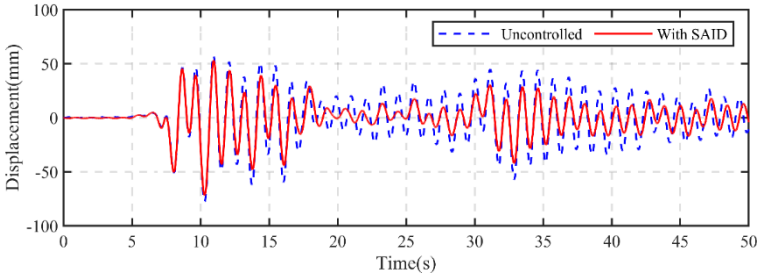

(a) Uncontrolled structure and structure with SAID attached

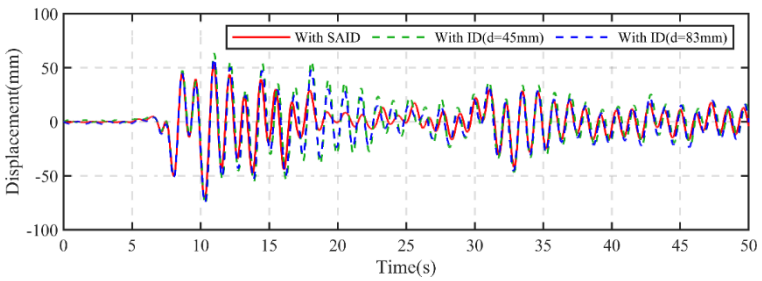

(b) Structures with SAID and passive ID attached

Fig. 14 Comparison of displacement time history curves

(a) Peak displacement (b) RMS displacement

Fig. 15 Comparison of vibration reduction ratio of structures with SAID or ID attached

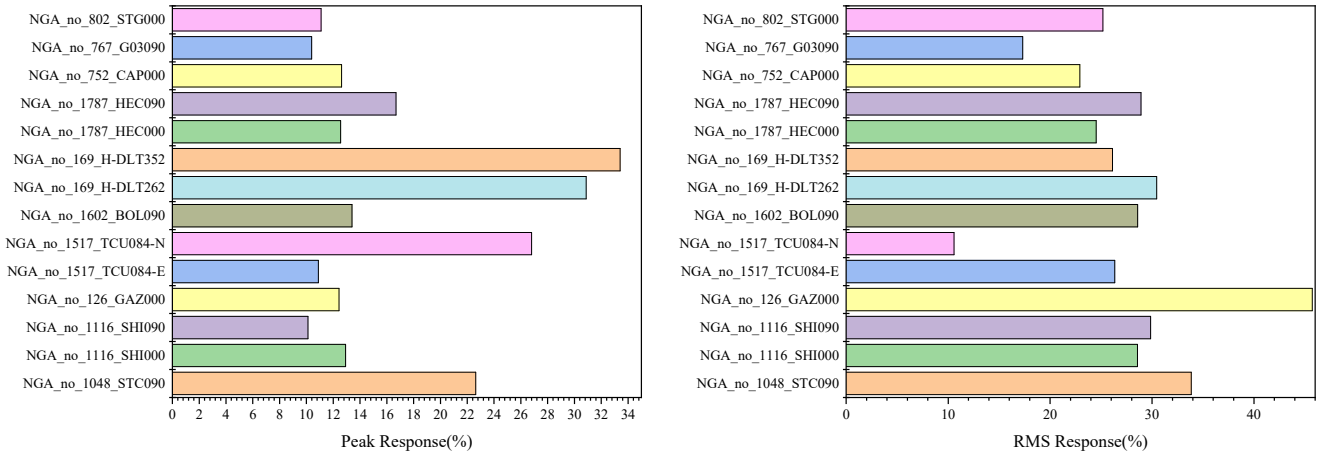

(a) Peak response (b) RMS response

Fig. 16 Displacement reduction ratios of SAID under different excitations

4.4 Comparison of SAID damping performance under different seismic excitation

To further explore the damping performance of SAID under unpredictable seismic excitation, the damping effect of SAID on structural displacements under different excitation is shown in Fig. 16. The damping effect of SAID on the peak displacement under the seismic excitation with different frequency characteristics remains mostly in the range of 10-14%, while the damping effect on the RMS of displacement remains basically in the range of 22-30%. This shows that the damping performance of SAID has good robustness under complex excitation environments.

5. Numerical simulation

5.1 Simulation model of SAID

Based on Eq. (1), a simulation model of SDOF structure with SAID attached is established in Simulink platform and MATLAB software. The semi-active control function is introduced to adjust the limited boundary positions by changing the values of d_1 and d_2, so as to realize the impact timing.

The parameter combination of the numerical simulation is kept the same as that in the experiment. The mass m, the natural frequency ω_n, and the damping ratio ξ of the SDOF structure are 9.13 kg, 0.891 Hz and 0.011, respectively. The mass ratio μ and impact damping ratio ξ_p of SAID device are 2.26% and 0.2, the impact frequency $\omega_p = 20\omega_n$. When the controlled structure is subjected to resonant harmonic excitation with an amplitude a_0 of 0.005 g and El Centro wave with an amplitude a_0 of 0.05 g, the time history curves of structural displacement and impact force are shown in Fig. 17, it is obvious that the impact forces always happen when the structural displacement is back to zero, which is consistent with the semi-active control strategy.

Fig. 18 represents the displacement time history curve of the structure with attached SAID compared to the optimal gap-clearance ID (Lu *et al.* 2011) under harmonic excitation. It can be observed that the two dampers can realize the similar control effect when they work in steady state; however, the SAID can start working and enter steady state quickly when compared with ID, leading to a stable vibration process. Consequently, the SAID shows better damping performance under harmonic excitation compared with ID.

5.2 Simulation model verification

To prove the accuracy of the simulation model, Fig. 19 compares the simulated and experimental results of the

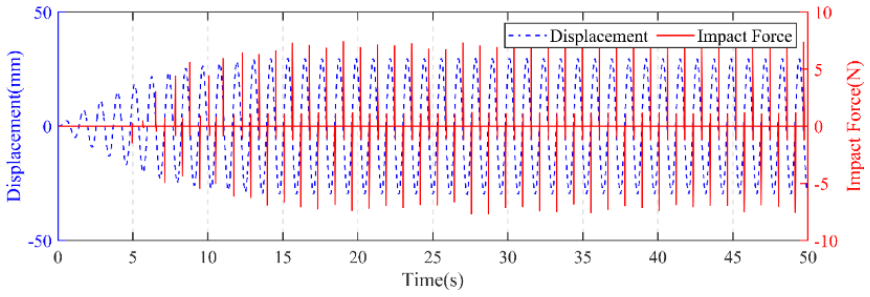

(a) Harmonic wave

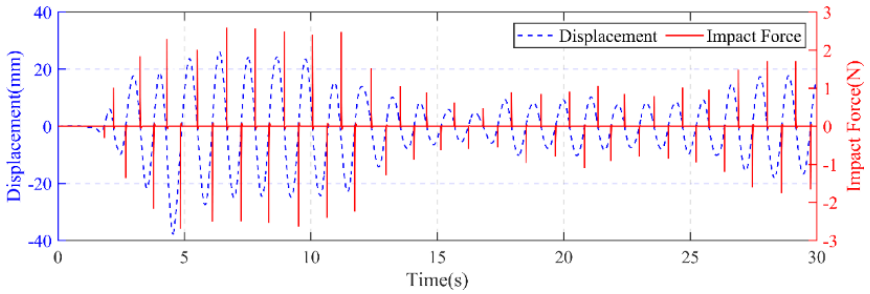

(b) El Centro wave

Fig. 17 Time history curves of structural displacement and impact force

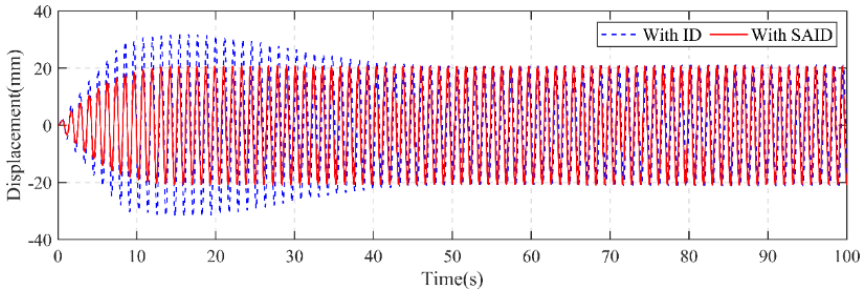

Fig. 18 Comparison of time history curves of structures with SAID and optimal ID attached

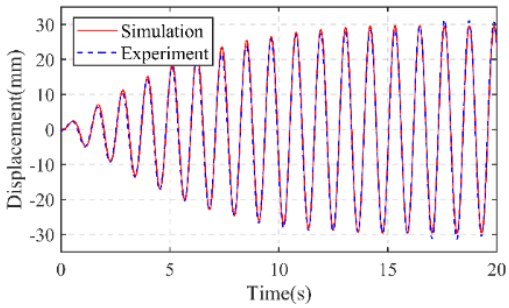

(a) Harmonic wave

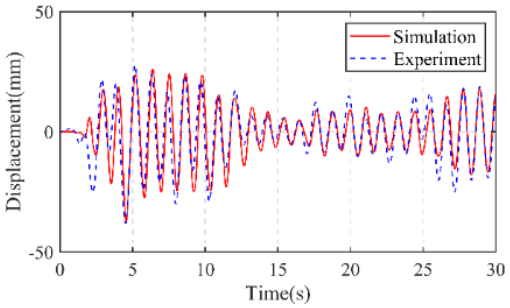

(b) El Centro wave

Fig. 19 Comprison of controlled structural displacement time history between simulated and experimental results

displacement time history of the test structures with SAID attached under harmonic (0.005 g) and El Centro (0.05 g) waves, corresponding to the working conditions B1 and C1 in Table 1. It can be observed that the structural displacement time history curves obtained from the numerical simulation agree well with that recorded from the experiment, indicating the effectiveness of the simulation model.

5.3 Parametric study

To further investigate the damping mechanism of SAID, a series of parametric studies have been conducted, including mass ratio μ, impact damping ratio ξ_p and excitation frequency ratio β. The frequency ratio refers to the ratio of the main frequency of the harmonic excitation to the natural frequency of the structure. The parameters of

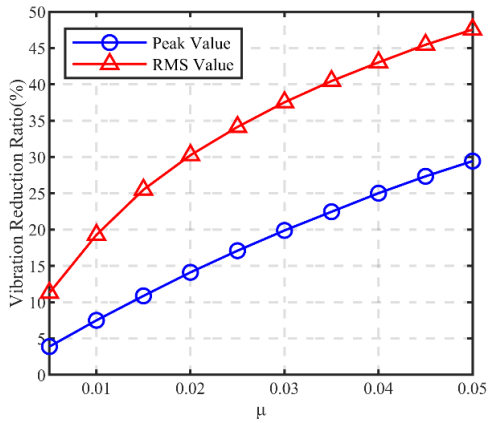

Fig. 20 The effect of SAID mass ratio on the SDOF structure under El Centro wave

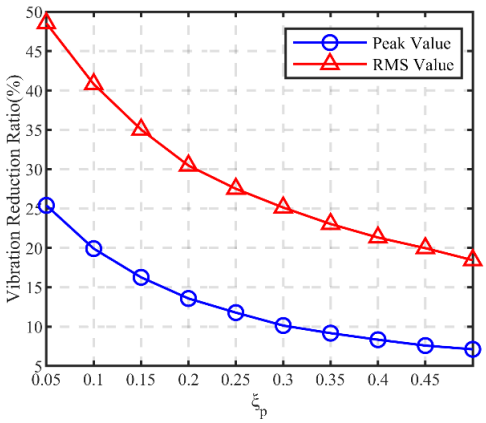

Fig. 22 The effect of SAID impact damping ratio on the SDOF structure under El Centro wave

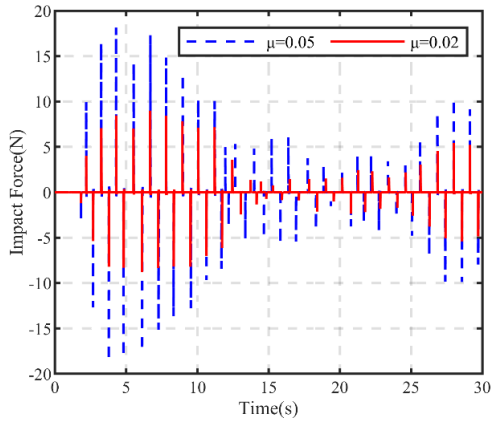

Fig. 21 Impact force from SAID with different mass ratios under El Centro wave

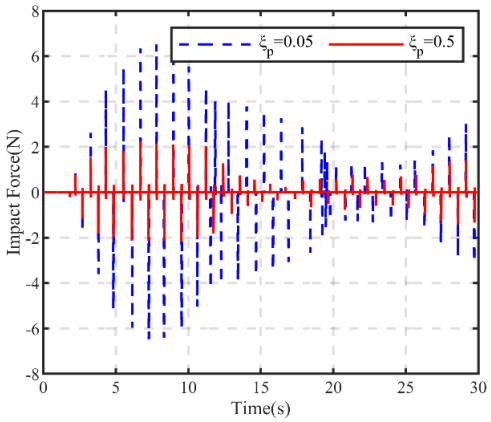

Fig. 23 Impact force from SAID with different impact damping ratios under El Centro wave

SAID are set as $\mu = 0.02$ and $\xi_p = 0.2$ initially.

5.3.1 Mass ratio

The influence of mass ratio on damping performance of SAID is shown in Fig. 20. It can be observed that the vibration reduction ratios of the controlled structure all increase with a larger mass ratio under El Centro wave. Fig. 21 compares the impact control forces of SAID with the mass ratio μ of 0.02 and 0.05, and it can be found that the impact block with higher mass can provide larger control forces under El Centro wave, resulting in better seismic attenuation effect.

5.3.2 Impact damping ratio

The effect of impact damping ratio on SAID damping performance is also studied and shown in Fig. 22. The variation of vibration reduction ratio with impact damping ratio is just opposite to that with mass ratio, that is, the vibration reduction ratios decrease and tend to be stable when the impact damping ratio of SAID rise from 0.005 to 0.5. Fig. 23 compares the impact force from SAID with impact damping ratio $\xi_p = 0.05$ and $\xi_p = 0.5$ when the controlled system is subjected to El Centro wave. When the impact damping ratio is lower, the impact block can move faster after one impact, providing sufficient control force

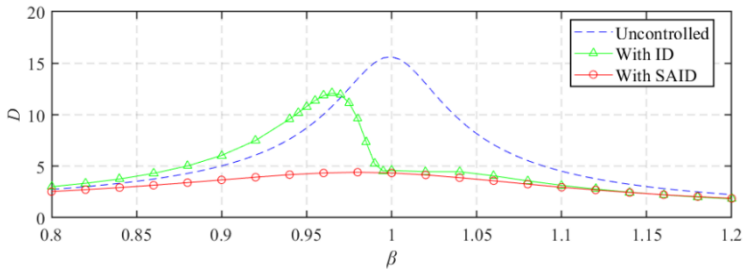

Fig. 24 Dynamic amplification factors for uncontrolled structure, ID controlled and SAID controlled structure

and efficient momentum exchange. Consequently, the effects of the parameters change on the damping effect of SAID is to change the impact force acting on the controlled structure essentially.

5.3.3 Excitation frequency ratio

To further explore the damping effect of SAID under different environments and structural characteristics, the dynamic amplification factor D, which represents the ratio of the harmonic response of the excited structure to its static response, is used as an indicator to study the vibration attenuation band of the SAID and ID with optimal gap-clearance. The effect of excitation frequency ratio on D is illustrated in Fig. 24. It can be seen that when the excitation frequency ratio is in the range $0.8 < \beta < 1.2$, the dynamic amplification factor D for the SAID controlled structure shows a wide damping band and stable damping performance compared to ID, which is unstable in the resonant state when $\beta < 1$.

6. Conclusions

In this paper, a semi-active impact damper (SAID) with a controllable impact timing strategy is proposed. The SAID mechanical device as well as the real-time monitoring feedback system is designed and fabricated, and the shaking table tests of the single shear frame with SAID and ID attached are carried out. The damping performance of SAID on the structure has been investigated by analyzing the shaking table test results, and the semi-active control strategy is also validated. The damping effect of SAID in the extreme working conditions under high-intensity excitation are discussed with that in the normal working conditions. Moreover, the damping performance of SAID under harmonic and seismic excitations is studied through numerical simulation. A series of parametric studies including mass ratio, impact damping ratio and excitation frequency ratio have been conducted to further investigate the damping mechanism of SAID, and obtained the following conclusions:

- The designed SAID can execute the preset semi-active control strategy well, and the damping performance will be affected in extreme conditions when the input excitation amplitude reaches a certain level limited by the design stroke. An appropriate increase of the maximum stroke and the slider-rail friction of the SAID can improve the damping performance of the SAID under strong excitation.
- The damping performance of SAID has good robustness under complex excitation environments. The damping effect of SAID under seismic excitation with different frequency characteristics is stable and efficient, with a vibration reduction ratio of 10-14% for peak response and 22-30% for RMS response.
- The proposed semi-active control strategy can improve the effective momentum exchange in impacts, thus enhancing the damping performance of the impact damping system. Under harmonic excitation, SAID can enter the steady state faster than the conventional passive impact damper. The numerical and experimental results show that SAID has a more stable damping effect than ID when the controlled system is subjected to harmonic and seismic excitations, indicating that SAID has a wider damping band and better robustness.
- The impact force is the key factor on the damping performance of SAID, an increase in the mass ratio and a decrease in the impact damping ratio allows the SAID system to provide greater impact control forces acting on the main structure, resulting in better vibration control effect.

Acknowledgments

Financial support from the National Natural Science Foundation of China (52178296) is highly appreciated. This work is also supported by Program of Shanghai Academic Research Leader (20XD1423900) and Top Discipline Plan of Shanghai Universities-Class I (20223YB15).

References

Chung, L.L., Lai, Y.A., Yang, C.S.W., Lien, K.H. and Wu, L.Y. (2013), "Semi-active tuned mass dampers with phase control", *J. Sound Vib.*, **332**(15), 3610-3625. https://doi.org/10.1016/j.jsv.2013.02.008

Domizio, M.N., Ambrosini, D. and Curadelli, O. (2019), "TMD effectiveness in nonlinear RC structures subjected to near fault earthquakes", *Smart Struct. Syst., Int. J.*, **24**(4), 447-457. https://doi.org/10.12989/sss.2019.24.4.447

Elias, S. and Matsagar, V. (2017), "Research developments in vibration control of structures using passive tuned mass dampers", *Annual Rev. Control*, **44**, 129-156. https://doi.org/10.1016/j.arcontrol.2017.09.015

Ferreira, F., Moutinho, C., Cunha, Á. and Caetano, E. (2019), "Use of semi-active tuned mass dampers to control footbridges subjected to synchronous lateral excitation", *J. Sound Vib.*, **446**, 176-194. https://doi.org/10.1016/j.jsv.2019.01.026

Gagnon, L., Morandini, M. and Ghiringhelli, G.L. (2019), "A review of particle damping modeling and testing", *J. Sound Vib.*, **459**, 114865. https://doi.org/10.1016/j.jsv.2019.114865

Gharib, M. and Karkoub, M. (2017), "Experimental investigation of linear particle chain impact dampers in free-vibration suppression", *J. Struct. Eng.*, **143**(2), 040161600. https://doi.org/10.1061/(ASCE)ST.1943-541X.0001638

Gur, S., Xie, Y. and DesRoches, R. (2019), "Seismic fragility analyses of steel building frames installed with superelastic shape memory alloy dampers: Comparison with yielding dampers", *J. Intell. Mater. Syst. Struct.*, **30**(18-19), 2670-2687. https://doi.org/10.1177/1045389X19873408

He, H., Wang, B. and Yan, W. (2021), "Mechanical Model and Optimization Analysis of Multiple Unidirectional Single-Particle Damper", *J. Eng. Mech.*, **147**(7), 04021040. https://doi.org/10.1061/(ASCE)EM.1943-7889.0001950

Hgsberg, J. (2011), "The role of negative stiffness in semi-active control of magneto-rheological dampers", *Struct. Control Health Monitor.*, **18**(3), 289-304. https://doi.org/10.1002/stc.371

Hrovat, D., Barak, P. and Rabins, M. (1983), "Semi-active versus passive or active tuned mass dampers for structural control", *J. Eng. Mech.*, **109**(3), 691-705.

https://doi.org/10.1061/(ASCE)0733-9399(1983)109:3(691)
Hwang, Y., Lee, C.W. and Jung, H.-J. (2020), "Feasibility of a new hybrid base isolation system consisting of MR elastomer and roller bearing", *Smart Struct. Syst., Int. J.*, **25**(3), 323-335. https://doi.org/10.12989/sss.2020.25.3.323
Iurasov, V. and Mattei, P.-O. (2020), "Bistable nonlinear damper based on a buckled beam configuration", *Nonlinear Dyn.*, **99**(3), 1801-1822. https://doi.org/10.1007/s11071-019-05387-7
Lai, Y.A., Chung, L.L., Yang, C.S.W. and Wu, L.Y. (2018), "Semi-active phase control of tuned mass dampers for translational and torsional vibration mitigation of structures", *Struct. Control Health Monitor.*, **25**(9), e2191.2191-e2191.2122. https://doi.org/10.1002/stc.2191
Ledezma-Ramírez, D.F., Tapia-González, P.E., Ferguson, N., Brennan, M. and Tang, B. (2019), "Recent advances in shock vibration isolation: An overview and future possibilities", *Appl. Mech. Rev.*, **71**(6), 060802. https://doi.org/10.1115/1.4044190
Lu, Z., Masri, S.F. and Lu, X. (2011), "Parametric studies of the performance of particle dampers under harmonic excitation", *Struct. Control Health Monitor.*, **18**(1), 79-98. https://doi.org/10.1002/stc.359
Lu, X., Zhang, Q., Weng, D., Zhou, Z., Wang, S., Mahin, S.A., Ding, S. and Qian, F. (2017), "Improving performance of a super tall building using a new eddy-current tuned mass damper", *Struct. Control Health Monitor.*, **24**(3), e1882. https://doi.org/10.1002/stc.1882
Lu, Z., Zhang, H. and Masri, S.F. (2019), "Studies on vibration control effects of a semi-active impact damper for seismically excited nonlinear building", *Smart Struct. Syst., Int. J.*, **24**(1), 95-110. https://doi.org/10.12989/sss.2019.24.1.095
Lu, Z., Zhang, J. and Wang, D. (2021), "Energy analysis of particle tuned mass damper systems with applications to MDOF structures under wind-induced excitation", *J. Wind Eng. Industr. Aerodyn.*, **218**, 104766. https://doi.org/10.1016/j.jweia.2021.104766
Ma, R., Bi, K. and Hao, H. (2021), "Inerter-based structural vibration control: a state-of-the-art review", *Eng. Struct.*, **243**, 112655. https://doi.org/10.1016/j.engstruct.2021.112655
Marano, G.C. and Greco, R. (2011), "Optimization criteria for tuned mass dampers for structural vibration control under stochastic excitation", *J. Vib. Control*, **17**(5), 679-688. https://doi.org/10.1177/1077546310365988
Marian, L. and Giaralis, A. (2017), "The tuned mass-damper-inerter for harmonic vibrations suppression, attached mass reduction, and energy harvesting", *Smart Struct. Syst., Int. J.*, **19**(6), 665-678. https://doi.org/10.12989/sss.2017.19.6.665
Masri, S.F., Miller, R.K., Dehghanyar, T.J. and Caughey, T.K. (1989), "Active parameter control of nonlinear vibrating structures", *J. Appl. Mech.*, **56**(3), 658-666. https://doi.org/10.1115/1.3176143
Nochebuena-Mora, E., Mendes, N., Lourenço, P.B. and Covas, J.A. (2021), "Vibration control systems: A review of their application to historical unreinforced masonry buildings", *J. Build. Eng.*, **44**, 103333. https://doi.org/10.1016/j.jobe.2021.103333
Papalou, A. and Masri, S. (1998), "An experimental investigation of particle dampers under harmonic excitation", *J. Vib. Control*, **4**(4), 361-379. https://doi.org/10.1177/107754639800400402
Parulekar, Y. and Reddy, G. (2009), "Passive response control systems for seismic response reduction: A state-of-the-art review", *Int. J. Struct. Stabil. Dyn.*, **9**(01), 151-177. https://doi.org/10.1142/S0219455409002965
Poplawski, B., Mikulowski, G., Pisarski, D., Wiszowaty, R. and Jankowski, L. (2019), "Optimum actuator placement for damping of vibrations using the Prestress-Accumulation Release control approach", *Smart Struct. Syst., Int. J.*, **24**(1), 27-35. https://doi.org/10.12989/sss.2019.24.1.027
Song, G., Zhang, P., Li, L., Singla, M., Patil, D., Li, H. and Mo, Y. (2016), "Vibration control of a pipeline structure using pounding tuned mass damper", *J. Eng. Mech.*, **142**(6), 04016031. https://doi.org/10.1061/(ASCE)EM.1943-7889.0001078
Soria, J.M., Diaz, I.M. and Garcia-Palacios, J.H. (2017), "Vibration control of a time-varying modal-parameter footbridge: study of semi-active implementable strategies", *Smart Struct. Syst., Int. J.*, **20**(5), 525-537. https://doi.org/10.12989/sss.2017.20.5.525
Sun, C. and Nagarajaiah, S. (2014), "Study on semi-active tuned mass damper with variable damping and stiffness under seismic excitations", *Struct. Control Health Monitor.*, **21**(6), 890-906. https://doi.org/10.1002/stc.1620
Wang, L., Nagarajaiah, S., Shi, W. and Zhou, Y. (2021), "Semi-active control of walking-induced vibrations in bridges using adaptive tuned mass damper considering human-structure-interaction", *Eng. Struct.*, **244**, 112743. https://doi.org/10.1016/j.engstruct.2021.112743
Xue, Q., Zhang, J., He, J., Zhang, C. and Zou, G. (2017), "Seismic control performance for pounding tuned massed damper based on viscoelastic pounding force analytical method", *J. Sound Vib.*, **411**, 362-377. https://doi.org/10.1016/j.jsv.2017.08.035
Yang, R., Zhou, X. and Liu, X. (2002), "Seismic structural control using semi-active tuned mass dampers", *Earthq. Eng. Eng. Vib.*, **1**(1), 111-118. https://doi.org/10.1007/s11803-002-0014-0

BS